Chin. J. Astron. Astrophys. Vol. 7 (2007), No. 6, 814–822
(*http://www.chjaa.org*)

Chinese Journal of
Astronomy and
Astrophysics

An Alternative Explanation for a Screw-like Meteoric Train Photographed by Double-Station Observations

Guang-Jie Wu[1,2]

[1] National Astronomical Observatories / Yunnan Observatory, Chinese Academy of Sciences, Kunming 650011; *yawugj@163.com*
[2] Purple Mountain Observatory, Chinese Academy of Sciences, Nanjing 210008

Received 2007 January 29; accepted 2007 March 26

Abstract Two-station observation of meteors, especially a meteor trains, provides an effective approach to the measurement of the physical parameters. We have collected four special groups of photographs of meteoric trains taken at two stations during Leonids 2001. One representative group has been measured and analyzed in detail. An analysis has been reported in our first paper. In this paper, an alternative explanation for the screw-like meteoric train is suggested based on some physical calculations. The results reveal that this train has a screw-like structure and, apparently, spoke beams. The mother meteor of this train may be negatively charged and moves forward along a left-hand screw trajectory under the effect of the geomagnetic field. The spoke beams might be the visual effect of the long time exposure of many particles released from the disintegrated meteoroid.

Key words: meteors, meteoroids — magnetic fields

1 INTRODUCTION

Meteoroids are the closest celestial bodies to us, but they are too tiny to be seen. In general, the diameter of a meteoroid is from only about 100 μm to several meters. In most cases we cannot observe the meteoroid itself, but only its radiation, but when a cosmic particle rushes into the Earth's atmosphere it is possible to see a meteoric event. Meteoric events are not rare, but the phenomenon is complex, including both physical and chemical processes. Especially, the characters of the persistent trains have not been understood very well (Jenniskens 2003; Jenniskens et al. 2000; Buchmann 2004; Wu & Zhang 2006).

We have organized the "2001 Leonid Meteor Shower Photograph Tournament" (abbreviated to 2001 LMSPT). Fortunately, the night of November 18/19 was clear. About 350 well-chosen photographs coming from all over the country were collected. Among them there are four special groups of photographs on the persistent meteoric trains. Each group was obtained by two different observers at different places. In despite of their having been taken by chance, they can still qualify as data of double-station observations (Wu & Zhang 2005). In our first paper, one representative group has been measured and analyzed on first view (Wu & Zhang 2006). Here, an alternative explanation for the screw-like meteoric train is suggested based on physical calculations.

2 OBSERVATIONS AND MEASUREMENTS

This typical group of photographs includes six pictures (see Fig. 1). In one observation a Phoenix DC901 camera with a 50 mm, f/1.8 lens was used, while a Seagull DF2 camera with a 50 mm, f/1.9 lens for another observation. Thus, the two cameras cover almost the same range of the field of view. It makes our measurement convenient and exact. In addition, Fuji Color film ISI 800 is used. In this paper six of the seven photographs are measured and the observational parameters are listed in Table 1.

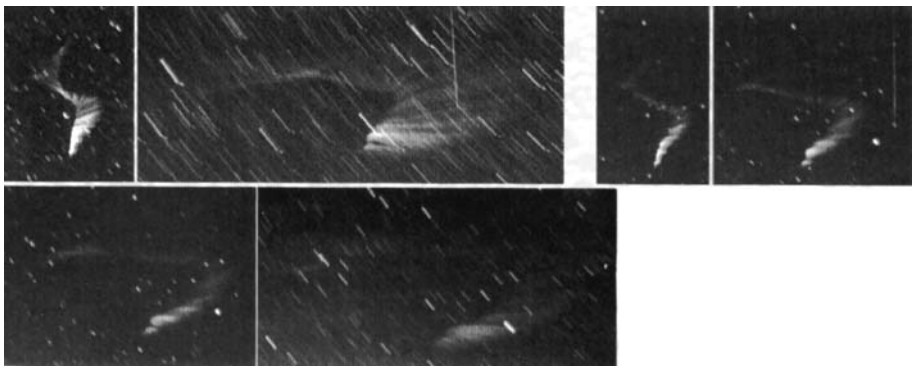

Fig. 1 A special meteoric train on six photographs obtained by two observers at different stations. From left to right: Nos. 186, 187, 347, 239, 348 and 349. All other parameters have been listed in Table 1.

Table 1 Parameters of the Photographs and Measurement Precision

No.	Obs. Time	Observer	Ref-Stars	α-Err(sec)	δ-Err(arcsec)	Cal. Exp. Time
186	05:19–05:20	J.D. Li	29	1.362	11.31	67.9 Sec.
187	05:20–05:25	J.D. Li	26	1.673	23.82	292.2
347	05:19–05:20	J.H. Yu	29	1.662	19.49	48.7
239	05:20–05:21	J.H. Yu	16	1.637	22.91	67.1
348	05:21–05:22	J.H. Yu	24	1.656	22.65	66.4
349	05:22–05:25	J.H. Yu	23	1.638	24.68	166.6

Table 2 Geographical Locations of Two Observers

Observer	Longitude	Latitude	Altitude
J.D. Li	$-116^\circ 49' 40.''81 \pm 0.''032$	$+40^\circ 33' 08.''07 \pm 0.''067$	162.8 ± 2.860 m
J.H. Yu	$-116^\circ 32' 12.''74 \pm 0.''052$	$+40^\circ 27' 15.''46 \pm 0.''052$	986.0 ± 1.414 m

The length of the exposure time of a certain photograph can be estimated directly, using the average length of the trails of a large selection of stars, as the camera was fixed. We found that the estimated time is nearly consistent with the time given by the observers. We list these values in the last column of Table 1, in units of seconds. For a given target, its position against the background star field can be easily measured. The number of the reference stars used in each photograph and the measurement errors in the directions of the longitude and latitude are also listed in Table 1.

In the measurement the time of observation is known so the azimuth and elevation of the target can be obtained. The radiant of the Leonids can be adopted as $\alpha = 154.^\circ 4, \delta = +21.^\circ 5$ (Suzuki et al. 2003). With the help of the Global Position System, the geographical locations of the two observing sites were measured after the event and listed in Table 2. The result shows the two observers were 26.9 km apart. All of our calculations are based on the spherical trigonometry of the earth-fixed coordinate system.

To reconstruct an integrated picture of the persistent train, we set several tens of diagnostic points on the train to finish the measurement. Usually, they are selected at the beginning and end of the "spoke" features as much as possible. These points are marked with the small squares in Figure 2, for an illustration..

Tables 3 and 4 list the measurements for the different points and different times in units of kilometer. The zero point of the coordinates is at the lower end of the train, which is near the diagnostic Point 1 (see Fig. 2) and the Z-axis points to the radiant of the Leonid. In fact, for convenience, in the local earth-fixed coordinate system the Z-axis points to the zenith and the X-axis points to east. In Table 3 the columns "5:19B" and "5:19E" represent the beginning and ending positions of a certain moving character point

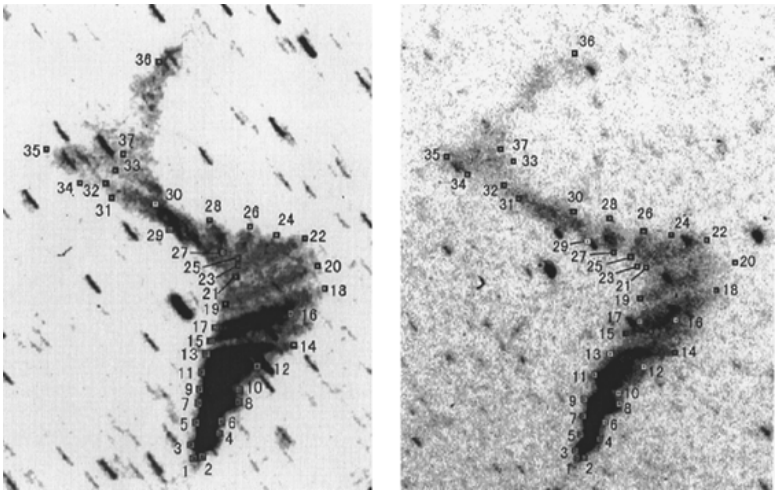

Fig. 2 Selected diagnostic points on the pair of photographs, Nos. 186 (left) and 347 (right).

on the photograph labelled with exposure time 5:19. Obviously, if we ignore the time gap between two successive exposures, then the ending point of a certain spoke should coincide with the beginning point of the same spoke in the next exposure. This means that the values "5:19E" and "5:20B" should be similar. So, their mean value and its average deviation are listed in the following columns under "Mean" and "Error". Similarly for the other pairs of values.

In our prime results, the errors in the X-direction have a mean value of 0.22 km and a rms deviation of 0.21 km. However, in the Y-direction they are over 10 times greater at 2.92 and 3.31 km, respectively. One important reason for this is the short distance between the two observers, since for a good double-station measurement, a distance about 60 to 100 km would be required (Koschny & Diaz del Rio 2002). Another reason is that a sizeable part of these errors comes from the ignoring of the time intervals between the successive exposures. In fact, we do not know how long this interval is. Especially, the lack of strict temporal coincidence in the exposures increased the difficulty in the selecting of the corresponding characteristic points in each pair of photographs and greatly increased the error of measurement. In comparison to the measuring accuracy of 10–25 arcsec for the reference stars, which corresponds to 0.012–0.030 km at about the distance of the train, the above errors are too large to be accepted. At least, some measurements with large errors should not be used, otherwise the resulting configuration of the train would be too complex and unreasonable. After omitting those measurements with errors greater than 2.5 km in the Y-direction, the remaining 17 points have a mean value of 0.17 km and a rms deviation of 0.20 km in the X-direction, 1.19 and 1.51 km in the Y-direction. These vetted points are used in constructing Figures 3 and 4.

Figures 3 and 4 show that: (1) Every diagnostic point almost keeps to a constant Z-value. For the whole 17 points their average movement in the Z-direction is only 0.512 km in the positive direction. (2) The envelope linking all the points at a certain time shows an outward and shifted movement on the $X-Y$ plane. Each diagnostic point moves with a nearly unchanged velocity. The whole envelope can be modelled as an elliptical loop at any time. Its major axis has an angle of about $-50\,^\circ$ by the X-axis. The size of the ellipse increases at a rate of about 83 m s^{-1} in the major-axis and of about 30 m s^{-1} in the minor-axis. Simultaneously, the center of the loop moves at an angle of about $+51\,^\circ$ to the X-axis and at a rate of about 32 m s^{-1}. Moreover, the train seems fashioned like a left-hand screw.

3 AN ALTERNATIVE EXPLANATION

In our last paper, an explanation was suggested that the persistent meteoric train might have been disturbed by the high altitude wind (Wu & Zhang 2006). Now, a meteoric train is easily disturbed by the high altitude wind. Jenniskens & Rairden (2000) thought that the "S"-shaped structure of the persistent train "Y2K" resulted from "a periodic wind variation" in the strong horizontal winds caused by gravity waves.

Table 3 Positions (1) of the Characteristic Points of the Train

Point	5:19B	5:19E	5:20B	Mean	Error	5:20E	5:21B	Mean	Error
$1X$	0.00	0.35	0.01	0.18	0.17	–0.35	–0.22	–0.29	0.07
$1Y$	0.00	0.85	0.02	0.44	0.42	–5.71	–6.46	–6.09	0.38
$1Z$	0.00	0.00	0.02	0.01	0.01	0.47	0.52	0.50	0.03
$3X$	–0.07	1.00	0.43	0.72	0.29	1.60	1.29	1.45	0.16
$3Y$	–0.23	1.75	1.54	1.64	0.11	7.44	11.38	9.41	1.97
$3Z$	0.43	0.67	0.47	0.57	0.10	0.00	–0.23	–0.12	0.12
$5X$	0.20	1.23	1.19	1.21	0.02	2.16	2.15	2.16	0.01
$5Y$	0.25	0.53	–0.84	–0.16	0.69	12.35	12.62	12.49	0.14
$5Z$	1.11	1.31	1.65	1.48	0.17	0.80	0.78	0.79	0.01
$7X$	0.38	1.88	1.17	1.52	0.36	3.19	2.57	2.88	0.31
$7Y$	1.12	1.49	0.17	0.83	0.66	10.65	19.66	15.16	4.51
$7Z$	1.77	1.92	2.16	2.04	0.12	1.62	1.04	1.33	0.29
$11X$	0.80	2.80	2.64	2.72	0.08	5.58	5.69	5.64	0.06
$11Y$	–2.38	–0.64	–1.97	–1.30	0.67	7.52	6.53	7.03	0.50
$11Z$	3.37	3.42	3.45	3.44	0.02	2.86	2.95	2.91	0.05
$13X$	1.40	4.07	4.14	4.10	0.04	7.73	7.72	7.73	0.01
$13Y$	–6.46	1.83	–6.26	–2.22	4.05	0.24	0.37	0.31	0.07
$13Z$	4.31	3.90	4.34	4.12	0.22	4.22	4.26	4.24	0.02
$15X$	1.99	4.20	4.91	4.56	0.36	8.28	8.38	8.33	0.05
$15Y$	–10.74	0.27	–3.75	–1.74	2.01	0.92	–0.18	0.37	0.55
$15Z$	5.11	5.19	5.03	5.11	0.08	5.21	5.35	5.28	0.07
$17X$	2.42	5.73	4.77	5.25	0.48	9.03	8.58	8.81	0.23
$17Y$	–13.04	–2.25	–5.92	–4.08	1.84	–16.54	–8.49	–12.52	4.03
$17Z$	5.66	6.28	5.63	5.96	0.33	7.21	6.56	6.89	0.33
$19X$	2.61	6.12	5.82	5.97	0.15	9.30	9.30	9.30	0.00
$19Y$	–9.99	–11.27	–8.52	–9.90	1.38	–6.65	–7.40	–7.03	0.38
$19Z$	6.42	7.52	7.17	7.34	0.18	8.19	7.61	7.90	0.29
$21X$	2.85	5.24	5.50	5.37	0.13	7.55	8.15	7.85	0.30
$21Y$	–8.14	–5.11	1.35	–1.88	3.23	1.22	–10.61	–4.70	5.92
$21Z$	7.41	8.31	7.84	8.08	0.24	8.77	9.13	8.95	0.18
$23X$	2.74	4.10	4.55	4.32	0.23	5.81	6.38	6.10	0.29
$23Y$	–3.56	–2.42	2.71	0.14	2.57	0.08	–9.68	–4.80	4.88
$23Z$	7.45	8.52	8.44	8.48	0.04	9.43	9.67	9.55	0.12
$25X$	2.50	3.08	3.32	3.20	0.12	4.04	5.27	4.66	0.62
$25Y$	–1.60	–1.81	7.63	2.91	4.72	1.09	–17.71	–8.31	9.40
$25Z$	7.72	8.76	8.62	8.69	0.07	9.48	10.01	9.75	0.27
$29X$		0.75				1.52			
$29Y$		–9.66				7.56			
$29Z$		8.94				9.04			
$35X$		–4.23				–8.58			
$35Y$		–2.41				3.81			
$35Z$		12.24				11.80			
$36X$	0.70		–2.09			–2.10			
$36Y$	–7.51		–1.84			–1.66			
$36Z$	15.51		13.81			13.83			
$37X$	–2.19		–5.24			–5.25			
$37Y$	5.82		2.45			2.60			
$37Z$	11.99		12.17			12.13			

Certainly, we often see a persistent train becoming disordered and disorganized. A very perfect screw-like train rarely appears in the literature, let alone having been carefully analyzed. The meteoric train "Y2K" had an unstable environment at least before 04:06. It was reflected on the lower half part of "Y2K" becoming gradually more trustworthy (Jenniskens & Rairden 2000). We notice that the atmospheric environment in our case is very different from "Y2K": Here, the atmosphere is much more stable. The persistent train can expand and diffuse placidly with an invariable velocity. Therefore, besides the gravity waves, we may need consider other possible factors.

Problems of turbulent plasma wakes of meteors have been discussed, and of the delicate geomagnetic pulses associated with meteor activities. It is well known that one of the first efforts to distinguish extrater-

Table 4 Positions (2) of the Characteristic Points of the Train

Point	5:21E	5:22B	Mean	Error	5:25
$1X$	–2.77	–3.69	–3.23	0.46	-0.37
$1Y$	11.31	22.76	17.04	5.73	4.98
$1Z$	–0.31	–0.70	–0.51	0.21	–0.29
$3X$	2.97	2.39	2.68	0.29	5.73
$3Y$	10.52	18.11	14.32	3.80	50.88
$3Z$	-0.54	–1.11	–0.83	0.29	–4.45
$5X$	4.06	3.50	3.78	0.28	8.03
$5Y$	15.42	23.44	19.43	4.01	69.37
$5Z$	–0.01	–0.68	–0.35	0.34	–4.76
$7X$	6.24	4.97	5.61	0.64	14.53
$7Y$	7.80	28.34	18.07	10.27	15.94
$7Z$	1.28	0.05	0.67	0.62	0.21
$11X$	9.30	9.31	9.31	0.01	20.52
$11Y$	8.12	8.47	8.30	0.18	15.21
$11Z$	2.84	2.80	2.82	0.02	2.67
$13X$	11.93	11.85	11.89	0.04	23.89
$13Y$	–4.18	–3.76	–3.97	0.21	1.04
$13Z$	5.07	5.05	5.06	0.01	6.24
$15X$	12.36				
$15Y$	–5.23				
$15Z$	6.03				
$17X$	12.53	12.52	12.53	0.01	22.71
$17Y$	–18.61	–19.04	–18.83	0.22	–23.92
$17Z$	7.58	7.60	7.59	0.01	9.62
$19X$	13.48	13.47	13.48	0.01	23.30
$19Y$	–25.61	–25.96	–25.79	0.18	0.61
$19Z$	8.98	8.99	8.99	0.01	10.20
$21X$	11.11	11.75	11.43	0.32	16.23
$21Y$	–32.89	–44.49	–38.69	5.80	–25.33
$21Z$	10.46	10.95	10.71	0.25	12.40
$23X$	7.74				
$23Y$	–15.55				
$23Z$	10.99				
$25X$	5.61	7.38	6.50	0.89	
$25Y$	–16.82	–44.66	–30.74	13.92	
$25Z$	11.05	11.95	11.50	0.45	
$29X$	1.84				
$29Y$	–3.16				
$29Z$	10.16				
$35X$	–14.35				–25.88
$35Y$	5.38				10.13
$35Z$	11.01				10.51
$37X$	–5.77				
$37Y$	3.98				
$37Z$	13.32				

restrial dust particles is based on their magnetic properties. The production of magnetite due to the heating during their entry into the atmosphere means that the geomagnetic field can have an evident effect on the ablated meteoroids (Whipple 1951; Jacchia 1955; Jones & Hawkes 1975; Hills & Goda 1993).

We deem that the screw-like train might be a result of diffusion of a spiral advance of the meteor. The description of "crawling-snake" meteors is indeed found in the historical literature and in the 2001 Leonids (Wu & Zhang 2003, 2005). Another reason is that the lowest spiral radius of about 5 km (see Fig. 4) needs about 1 minute to travel at the velocity of 83 m s^{-1}. However, the first exposure is only about 10–20 second after the mother meteor appeared. It requires that the path of the mother meteor should not be a straight line but one with an initial radius. Reason three, all the characteristic points have almost no velocities in the radiant direction while having certain initial velocities perpendicular to the radiant direction. These perpendicular movements could be a reflection of the interaction of a charged meteoroid with the geomagnetic field.

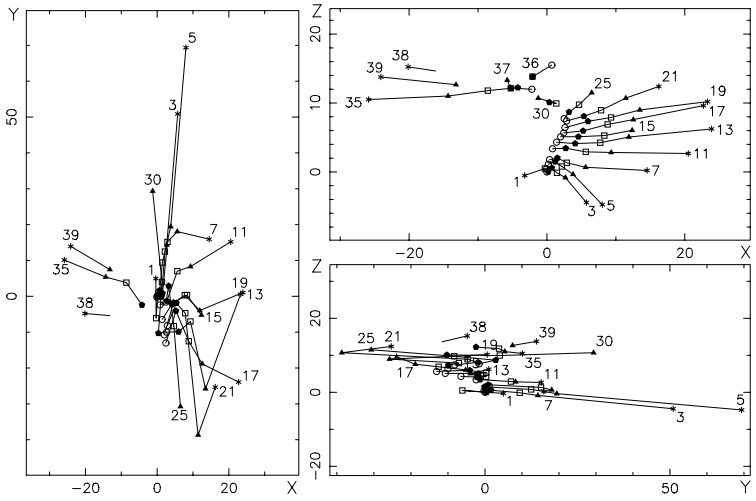

Fig. 3 Individual movements of the selected diagnostic points.

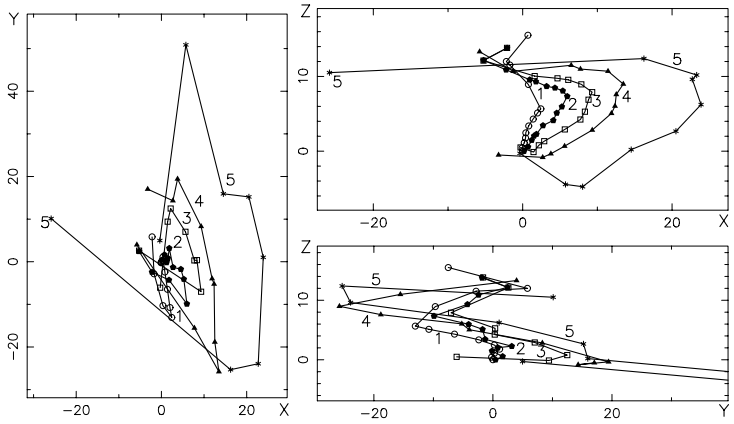

Fig. 4 Whole movements of the selected diagnostic points as an envelope at any certain time.

In all of our following calculations, the MKSA system of electromagnetic units is used, in which the charge-to-mass ratio for an electron is

$$[Q/M]_{\rm e} = \frac{1.6 \times 10^{-19}\ {\rm C}}{9.1 \times 10^{-31}\ {\rm kg}} = 1.76 \times 10^{11}\ [{\rm C\ kg^{-1}}], \tag{1}$$

and that for a proton is

$$[Q/M]_{\rm P} = \frac{1.6 \times 10^{-19}\ {\rm C}}{1.67 \times 10^{-27}\ {\rm kg}} = 9.58 \times 10^{7}\ [{\rm C\ kg^{-1}}]. \tag{2}$$

For the total charge production during a hyper-velocity impact of a meteor an empirical formula was found as

$$Q = 3.04\delta^{1.02} r^{3.06} v^{3.48}\ [{\rm C}], \tag{3}$$

where δ is the meteoric density [kg m^{-3}], r the meteoroid's radius [m] and v the speed [km s^{-1}] (McBride & McDonnell 1999; Foschini 2002). We can rewrite the formula as

$$Q = 0.70525 M^{1.02} v^{3.48}\ [{\rm C}], \tag{4}$$

where M is the mass of the meteoroid in units of [kg]. Therefore, for the Leonids it should be, roughly,

$$[Q/M]_{\rm L} \simeq 0.70525 \times (71.9)^{3.48} = 2.04 \times 10^6 \ [{\rm C\ kg^{-1}}]. \tag{5}$$

In fact, another empirical formula,

$$\log M = 5.15 - 0.44 m_{\rm ph} - 3.89 \log v - 0.67 \log(\sin(h_r))\,, \tag{6}$$

can be also used (Jenniskens 1999; Zhang & Wu 2002), where M is the meteoric mass [g], $m_{\rm ph}$ the meteoric photometric magnitude, v the speed [km s^{-1}] and h_r the elevation of the shower's radiant at the time of the observation. For this paper, h_r is $64.^\circ5475$. In virtue of Equations (4) and (6), an accurate calculation gives the $[Q/M]_{\rm L}$ ratio from 1.46×10^6 to 2.10×10^6 C kg^{-1} in the magnitude range $m_{\rm ph} = +5 \sim -13$. This result is well consistent with Equation (5).

A moving electrified body in a magnetic field will follow a circular movement. In the MKSA system the Lorentz force is

$$F = Q \cdot v \cdot B \cdot \sin\alpha = M\frac{v_\perp^2}{R}, \tag{7}$$

where B is the intensity of the magnetic field, α the tilt angle of the moving direction of the body to the magnetic field, R and $v_\perp$ the radius and the tangential velocity of the circular movement, respectively, in the $X-Y$ plane. So, we have

$$[Q/M] = \frac{v_\perp^2}{R \cdot v \cdot B \cdot \sin\alpha}. \tag{8}$$

Adopting $(78.^\circ7N,\ 70.^\circ5W)$ as the position of the geomagnetic northern pole, the observing site has geomagnetic longitude $-6.^\circ27$, and latitude $+29.^\circ28$, intensity $B = 5.3 \times 10^{-5}$ T, magnetic deflection angle $+1.^\circ61$ north by east and magnetic obliquity $+48.^\circ27$. In addition, a Leonid meteor has an angle of $\alpha = +151.^\circ17$ to the direction of the geomagnetic field.

So, for the meteor moving a distance of about 15.5 km with a velocity of 71.9 km s^{-1} along its trajectory in a nearly circular movement of radius R, we have

$$\frac{2\pi R}{v_\perp} = \frac{15.5}{71.9}. \tag{9}$$

Two special situations can be calculated. Since the lowest spiral radius in Figure 4 is about 5 km, adopting $R < 5$ km, we have

$$v_\perp < 71.9 \times \frac{10\pi}{15.5} = 145.7\ {\rm km\ s^{-1}}\,, \tag{10}$$

and

$$[Q/M]_1 < \frac{(145.7)^2}{5 \times 71.9 \times 5.3 \times 10^{-5} \cdot \sin(151.^\circ173)} = 2.3 \times 10^6\ [{\rm C\ kg^{-1}}]. \tag{11}$$

If we adopt the outward velocity of the loop as $v_\perp = 83$ m s^{-1}, we have

$$R = \frac{0.083}{2\pi} \cdot \frac{15.5}{71.9} = 0.00285\ [{\rm km}], \tag{12}$$

and

$$[Q/M]_2 = \frac{(0.083)^2}{0.00285 \times 71.9 \times 5.3 \times 10^{-5} \cdot \sin(151.^\circ173)} = 1317\ [{\rm C\ kg^{-1}}]. \tag{13}$$

Therefore, the following relationship can be found

$$[Q/M]_{\rm e} \gg [Q/M]_{\rm P} \gg [Q/M]_{\rm L} \simeq [Q/M]_1 \gg [Q/M]_2. \tag{14}$$

It means that a huge number of combinations of the electrons and protons can satisfy the charge state of the Leonids. Moreover, the ratio $[Q/M]_{\rm L}$ of the Leonids meteors, or the size of the charge per unit mass, can meet the requirements of a supposed spiral movement of the meteor. However, the positive or negative electricity of a meteor can not be determined solely by the amount of the charge. Studies have indicated that the meteoroids in the magnetosphere can be negatively charged in a cold plasma, or switch their charges to positive values (Horanyi 1996, 2000; Foschini 2002). In this paper, the left-hand screw forward of the train suggests that it should be negatively charged.

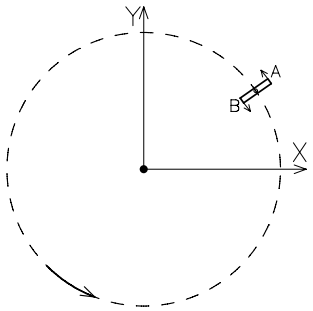

Fig. 5 A sketch of the meteoroid's movement, which makes the screw-like train. The Z-axis points to us.

4 DISCUSSION

In general, meteoric phenomena take place at height between 80–100 km, the E-layer of the ionosphere. Meteoric trains at this height can be often distorted by the high-altitude winds. However, among our collected photographs, in the E-layer of the ionosphere there is the phenomenon of the "snake-crawl" meteor, which is impressive and known to be recorded already in ancient Chinese documents (Wu & Zhang 2003, 2005). We think that the "snake-crawl" behavior of a meteor may be a reflection of the interaction of the charged meteoroid with the geomagnetic field. Being acted upon by both the Lorentz force and gravitational force, a meteoroid may move along a spiral line. The spiral train in a quiet atmosphere may have some inherent relationship with the "snake-crawl" meteor. The snake-like curve in a 2-dimensional plot should be the projection of a screw-like curve in three dimensions. At any given time, the screw-like train has just an "S"-shape trace, looking like a one-periodic snake moving, and expanding perpendicularly outwards all the time. The spokes on the photographs are results in a long exposure. It is a pity that up to now few photographs like these are found in literature. The most clear photograph of a spiral train was captured by Qi-sheng Lin in the 2001 Leonids (Wu & Zhang 2005, 2006).

In this paper, a long-lasting train observed at two stations showed a very clear screw-like structure with spoke beams. Each spoke looks like nearly perpendicular to the axis of the screw-like surface. Generally, there are several tens of spoke beams in a screw-like train. Therefore, the period is on the general order of 0.01 second. We think this sort of train occurs at stable environments free or nearly free from the random effects of the high altitude winds.

Since most meteor streams come from comets, the "dustball" model naturally suggests that a meteoroid should be a porous and fragile aggregate of many small particles stuck together by a kind of "glue" with a low boiling point (Hawkes & Jones 1975; Jacchia 1955). In the first stage of the ablation of the meteoroid, the "glue" melts and the meteoroid releases grains, with diameters of about 200–300 μm.

Therefore, we think the spokes in the screw-like train come from the spin of the original meteoroid. A sketch is suggested in Figure 5. The centrifugal force of the screw-like movement may make the ablated meteoroid to be a short bar athwart the $X-Y$ plane. As a result of both the revolution and rotation, while the spinning bar points to the Z-axis, the outer end 'A' falls under the maximum effect of the centrifugal forces. As a result, it is possible to release one (or more) particle(s) of the "dustball" at that time. As the whole meteor bar moves and spins, the release occurs periodically. The outward movement of each particle makes a spoke-like trace in the long time exposure photograph. Hawkes & Jones (1978) thought that if the meteoroids were initially rotating about the trajectory axis, the mean angular velocity ω might be up to 5000 rad s^{-1}. In this paper, a period of 0.01 s only corresponds to about $\omega = 300 - 600$ rad s^{-1}, which is much lower and easy to be satisfied.

Acknowledgements The author thanks the anonymous referee for his/her helpful and perceptive advice and comments. The author is very grateful to Mr. Jun-Duo Li, Mr. Jie-Hong Yu, Mr. Zhou-Sheng Zhang and to Prof. Chong-Yi Gao of the Lanzhou University for their kind supports and help.

References

Buchmann A., 2004, WGN, the journal of the IMO, 32(1), 23
Foschini L., 2002, In: E. Murad et al., eds., Meteors in the Earth's atmosphere, Cambridge: Cambridge Uni. Press, 249
Hawkes R. L., Jones J., 1975, MNRAS, 173, 339
Hawkes R. L., Jones J., 1978, MNRAS, 185, 727
Hills J. G., Goda M. P., 1993, AJ, 105, 1114
Horanyi M., 1996, Annu. Rev. Astron. Astrophys., 34, 383
Horanyi M., 2000, Phys. Plasmas, 7, 3847
Jacchia L. G., 1955, AJ, 121, 521
Jenniskens P., 1999, Laboratory Astrophysics and Space Research, Netherlands, 425
Jenniskens P., 2003, WGN, the journal of the IMO, 31, 88
Jenniskens P., Rairden R., 2000, Earth, Moon and Planets, 82, 457
Jenniskens P., Lacey M., Allan B. et al., 2000, Earth, Moon and Planets, 82, 429
Jones J., Hawkes R. L., 1975, MNRAS, 171, 159
Koschny D., Diaz del Rio J., 2002, WGN, the journal of the IMO, 30, 87
McBride N., McDonnell J. A. M., 1999, Planet. Space Sci., 47, 1005
Suzuki S., Akebo T., Suzuki K. et al., 2003, WGN, the Journal of the IMO, 31, 183
Whipple F. L., 1951, ApJ, 113, 464
Wu G.-J., Zhang Z.-S., 2003, Chin. Astro. Astroph., 27, 435
Wu G.-J., Zhang Z.-S., 2005, Astronomical Research & Technology, 2, 60
Wu G.-J., Zhang Z.-S., 2006, New Astronomy, 12, 104
Zhang Z.-S., Wu G.-J., 2002, Chin. Astro. Astroph., 26, 208